TECHNICAL PAPER

Effect of interference fit on dynamic characteristics of spindle rotor system

Zinan Wang[1] · Zhan Wang[1] · Xiaotian Bai[1] · Xiaochen Zhang[1] · Yonghua Wang[1]

Abstract

The interference fit of the front and rear bearings inner rings have a significant effect on dynamic characteristics of spindle rotor system. In order to study the interference amount variation of bearing inner ring under different working conditions, a bearing interference fit model is established considering centrifugal displacement and thermal displacement. The temperature simulation model of spindle is proposed, which can analyze the relationship between temperature and thermal displacement. Newton iteration method is utilized to solve the bearing dynamic model, and the interference effect on dynamic characteristics of the bearing has been explored in detail. The results reveal that the bearing inner ring initial interference will tend to decrease with the increase of speed, and the influence of temperature and centrifugal force are significant. In addition, the reliability of the proposed model is verified by different temperature and vibration experiments. Under high speed condition, the interference amount between bearing and shaft should be appropriately increased. The bearing interference fit research is helpful for the dynamic characteristics analysis of bearing, which can be considered as a guide in spindle rotor system fit mode.

Keywords Spindle rotor system · Bearing · Interference fit · Displacement · Dynamic characteristics

1 Introduction

With the rapid development of precision manufacturing technology, the dynamic characteristics requirements of numerical control machine tool spindle is becoming increasingly higher. In order to ensure the output quality of spindle, the interference fit is adopted between shaft and the bearing in spindle. Due to the influence of dynamic and thermal characteristics, the radial displacement of the bearing have a great effect on the interference amount variation, even making the interference fit into transitional fit or clearance fit [1–4]. For actual bearing dynamic behavior, interference amount directly affects the vibration of bearing [5, 6]. If the interference amount is larger, it will enhance the matching pressure, then resulting in the matching surface appears slip phenomenon. And it even may lead to destroying the

matching surface. If the interference amount is smaller, the wear and temperature of the shaft and bearing may lead to rising. Therefore, the research on the interference fit of bearing dynamic behavior is significant. In recently years, the relevant fields of spindle rotor system interference fit have attracted research scientists' attention. Some related achievements have been achieved through many methods. Liu et al. proposed interference fit modified spindle rotor system model considering assembly deformation and centrifugal expansion factors, which can predict different interference fit values [7]. Gruescu et al. analyzed interference fit amount with the vector composition law of axial and tangential direction loadings through FEM [8]. Barmanov et al. calculated and revealed the influence of bearing ball interference fit with radial, axial displacements of the bearing rings through numerically iterations method [9]. Tsai et al. analyzed the contact pressure distribution and stiffness variation between the shaft and the bearing, and the interference amount is considered [10]. Mao et al. constructed a modified dynamic bearing model which can analyze the ring deformation effect on the clearance fit with bearing housing, and drawing a conclusion that a small fit clearance amount can improve the dynamic characteristics of bearing [11].

✉ Zhan Wang
juven1126@163.com

1   School of Mechanical Engineering, Shenyang Jianzhu University, Shenyang 110168, China

Chen et al. carried out a dynamic spindle model through the finite element method, which can evaluate the relationship between the interference fit and spindle stiffness [12]. Although some general methods of bearing assembling fit models have been investigated, the dynamic interference amount is only one of the common influence factors in spindle rotor system dynamic behavior.

Because the bearing interference fit amount is also affected by temperature. Some temperature field effect on the bearing fit methods had been presented in relevant work. Shi et al. had proposed a calculation vibration method for the ceramic bearing which the thermal deformation difference was considered, and made a decision that the bearing fit had an obvious impact of the dynamic characteristics of ceramic bearing [13]. Bai et al. proposed a ceramic bearing dynamic model which the temperature-related fit clearance is considered, the relationships between the temperature, fit and vibration were explored [14]. Murčinková et al. focused radial stress, radial displacement and other parameters on the interference change of the press fit on bearing-shaft joint [15]. Guo et al. developed the interference fit bearing model for analyzing interference fit amount have a great impact on the dynamic characteristics of spindle, which considering the influence of rotational speed and the temperature[16]. However, the above research results have obtained encouraging ideas, the influence of centrifugal displacement and thermal displacement act on the bearing fit together which are often overlooked.

On the basis of the existing research, the bearing dynamic displacement, centrifugal displacement and thermal displacement are closely relevant to the bearing interference fit amount. In order to reflect the relationship between the temperature and bearing interference amount, a temperature field model is proposed. Then, due to the influence of the interference amount variation, the bearing dynamic model is established to analyze the bearing nonlinear behaviors. Lastly, the spindle rotor system temperature and vibration simulation analysis results are verified through experiments. The theoretical research on the bearing interference fit can provide the technical support for the fit mode of spindle rotor system.

2 Spindle rotor system interference fit model

2.1 Calculation of spindle rotor system interference amount

The fit mode of the spindle rotor system adopts interference fit, which directly affects the deformation of the bearing inner ring. The outer ring of the bearing and the bearing seat are fixed as a stationary ring. The 7008C and 7009C angular contact ball bearings are used in the spindle. The bearing structure is shown in Fig. 1.

According to the fit size table, the tolerance band of the shaft is K5, the shaft at the installation place of front bearing 7009C is $45^{+0.013}_{+0.002}$, the size of the front bearing inner ring is $45^{0}_{-0.012}$; the installation place of rear bearing 7008C is $40^{+0.013}_{+0.002}$, and the size of rear bearing is $40^{0}_{-0.012}$. The deformation generated by the bearing will lead to bearing inner raceway varying. If the pressure is uniformly applied to the inner circumference, or the outer circumference and the wall thickness exceeds 20% of the diameter, it is regarded as a thick-walled ring. Under the influence of the assembly stress, the interference relationship is shown in Eq. (1).

$$\Delta f = |\Delta_i| + |\Delta_s|, \tag{1}$$

where Δf is the total interference (μm), Δ_s is the single side interference of shaft (μm), Δ_i is the single side interference of inner ring (μm).

Under the influence of the initial interference amount, the bearing inner ring raceway will undergo deformation as shown in Eq. (2).

$$\delta_{F2} = \frac{d}{d_i} \cdot \frac{1 - \left(\frac{d_0}{d}\right)^2}{1 - \left(\frac{d_0}{d_i}\right)^2} \Delta f, \tag{2}$$
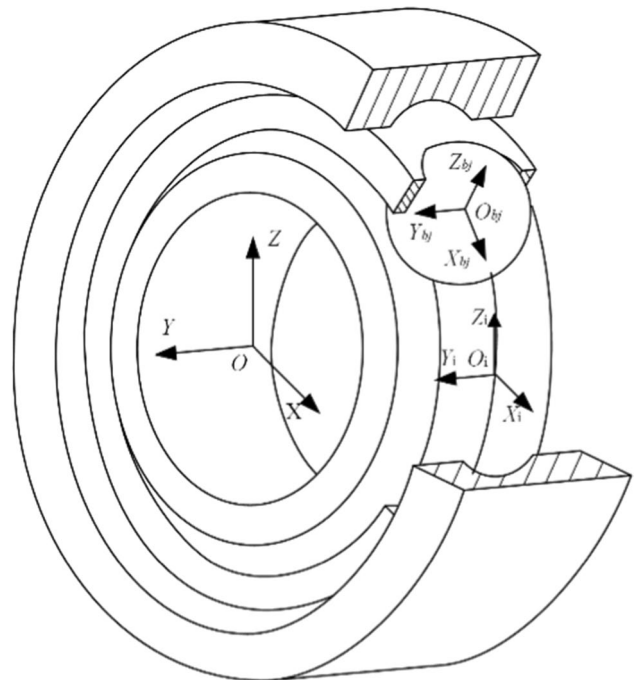

Fig. 1 The bearing structure

where d is diameter of bearing inner ring (mm), d_i is diameter of bearing inner ring outer raceway (mm), d_o is diameter of shaft inner hole (mm).

The structural variation of bearing and shaft is shown in Fig. 2.

The connection between the bearing and the shaft generally adopts the expansion and contraction method. The minimum combined pressure for transmitting load is shown in Eq. (3).

$$p_{f\,min} = \frac{F_a}{\pi d_f l_f u}, \tag{3}$$

where F_a is axial force (N), d_f is assembly diameter (mm), l_f is assembly length (mm), u is friction coefficient of shaft friction pair.

According to the variation of the minimum diameter, the calculation of the minimum interference is shown in Eq. (4).

$$\Delta f_{min} = \Delta f_{a\,min} + \Delta f_{i\,min},$$
$$\Delta f_{a\,min} = p_{f\,min} d_f \frac{C_a}{E_a}, \tag{4}$$
$$\Delta f_{i\,min} = p_{f\,min} d_f \frac{C_i}{E_i},$$

where $\Delta f_{a\,min}$ is minimum interference on single side of bearing inner ring, $C_a = \frac{1+q_a^2}{1-q_a^2} + \mu_a$, $q_a = \frac{d_f}{d_a}$ is the diameter ratio of the bearing, $\Delta f_{i\,min}$ is minimum interference on single

side of shaft, $C_i = \frac{1+q_i^2}{1-q_i^2} - \mu_i$, $q_i = \frac{d_0}{d_f}$ is the diameter ratio of the shaft.

The maximum interference ensures that the bearing and the shaft cannot produce plastic deformation. It is necessary to calculate the maximum allowed pressure between the joint surfaces without plastic deformation, as shown in Eq. (5).

$$p_{fa\,max} = \frac{1 - q_a^2}{1 + q_a^2} \times \frac{\sigma_{ba}}{3},$$
$$p_{fi\,max} = \frac{0.4\sigma_{bi}}{2}, \tag{5}$$

where σ_{ba} is tensile strength of bearing inner ring (MPa), σ_{bi} is tensile strength of shaft (MPa).

According to the variation of the maximum diameter, the maximum interference is calculated as shown in Eq. (6).

$$\Delta f_{max} = \Delta f_{a\,max} + \Delta f_{i\,max},$$
$$\Delta f_{a\,max} = p_{fa\,max} d_f \frac{C_a}{E_a}, \tag{6}$$
$$\Delta f_{i\,max} = p_{fi\,max} d_f \frac{C_i}{E_i},$$

where Δf_{amax} is maximum interference on single side of bearing inner ring, Δf_{imax} is maximum interference on single side of shaft.

The calculated minimum interference and maximum interference are required for the bearing can fit with the shaft, the basic interference amount is shown in Eq. (7).

$$\Delta f_b = \frac{\Delta f_{min} + \Delta f_{max}}{2}. \tag{7}$$

According to Eqs. (3–7), the interference of the rotor system is between 0.002 mm and 0.025 mm, which does not exceed the theoretical maximum range.

2.2 Thermal deformation effect on the interference amount

Bearing will generate a large amount of heat during spindle operation. The heat will increase the spindle rotor system temperature, thus thermal displacement generated can cause the variation of the interference amount. The thermal displacement of the bearing inner ring and the shaft leads to interference amount varying [17, 18]. Under the effect on thermal displacement, the interference fit relationship between the bearing inner ring and the shaft is shown in Fig. 3. Because the shaft and the bearing inner ring can generate thermal displacement, the interference amount is shown in Eq. (8).

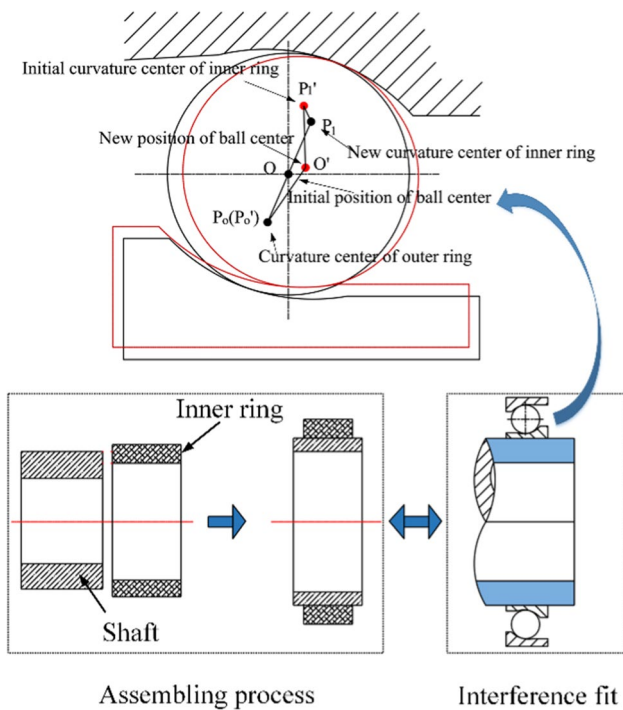$$\Delta f = \Delta_s + \Delta_i + u_i - u_s, \tag{8}$$

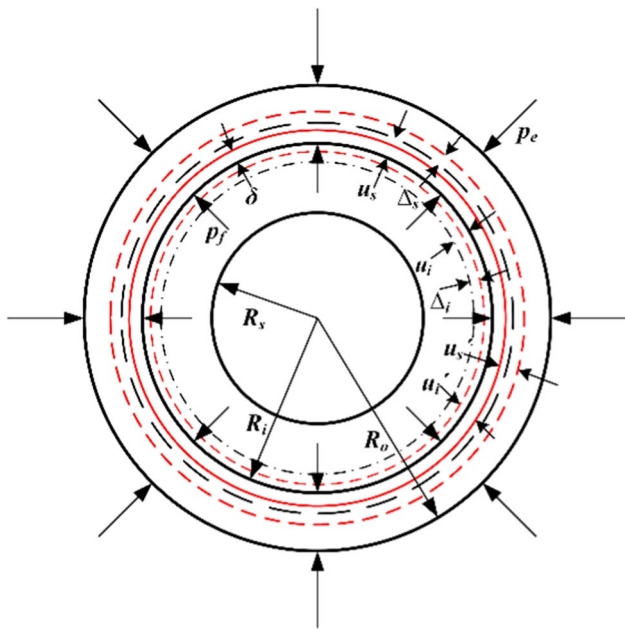Fig. 2 The structural variation of bearings and shaft

Fig. 3 The interference fit relationship of bearing and shaft

where u_s is radial thermal displacement of shaft (μm), u_i is radial thermal displacement of bearing inner ring (μm).

The bearing is simplified as an axis symmetric ring, and the bearing seat and the shaft are simplified as a bearing long cylinder. The calculation of radial thermal displacement of the shaft and bearing is shown in Eq. (9) [19].

$$u_s = \alpha_s \Delta T_s (1 + \mu_s) d,$$
$$u_i = \alpha_i \Delta T_i d, \tag{9}$$

where α is thermal expansion coefficient of bearing (mm/°C), ΔT is temperature rise (°C).

The change of shaft and bearing inner ring interference caused by temperature rise is shown in Eq. (10).

$$\Delta f_T = u_i - u_s = \left[\alpha_i \Delta T_i - \alpha_s \Delta T_s (1 + \mu_s) \right] d. \tag{10}$$

2.3 Centrifugal force effect on the interference amount

When the spindle rotates at high speed, the inner ring diameter of the bearing and the outer diameter of the shaft expand under the action of centrifugal force. The centrifugal displacement of the shaft increases the interference on the matching surface, while that of the bearing inner ring reduces. The expansive appearance may reduce the matching stress and interference amount on the matching surface, which may appear the matching surface appears slip phenomenon. The radial displacement of the bearing inner ring raceway, the inner diameter of the bearing inner ring and the

outer diameter of the shaft under centrifugal force are shown in Eq. (11) [20].

$$u_{i1} = \frac{(1 - \mu_i)d_i^3 + (3 + \mu_i)d_i d^2}{32E_i} \rho_i \omega^2,$$

$$u_{i2} = \frac{(1 - \mu_i)d^3 + (3 + \mu_i)d d_i^2}{32E_i} \rho_i \omega^2, \tag{11}$$

$$u_{s1} = \frac{(1 + \mu_s)\left[(3 - 2\mu_s)d d_0^2 + (1 - 2\mu_s)d^3\right]}{32E_s} \rho_s \omega^2,$$

where u_{i1} is the centrifugal displacement of bearing inner ring raceway (μm), u_{i2} is the centrifugal displacement of bearing inner ring (μm), u_{s1} is the centrifugal displacement of shaft, ρ_i is the material density of bearing inner ring, ω is speed (r/min), E_i is the elastic modulus of bearing inner ring (MPa), E_s is the elastic modulus of shaft (MPa).

The change of the interference caused by the centrifugal displacement is shown in Eq. (12).

$$\Delta f_c = u_{i2} - u_{s1}. \tag{12}$$

2.4 Dynamic displacement of bearing effect on the interference amount

The dynamic radial displacement of the bearing in the rotation process is also the main reason for the bearing dynamic behavior [21]. Combined with the quasi-statics theory of bearings, the contact angle of bearing inner ring is correlated with interference amount. The force between the inner, outer ring and the ball is shown in Fig. 4. The force model of the bearing are shown in Eqs. (13) and (14).

$$F_x + \sum_{j=1}^{z} (Q_{ij}\sin\alpha_{ij} - F_{R\eta ij}\cos\alpha_{ij}) = m_i\ddot{x}_i,$$

$$F_y + \sum_{j=1}^{z} \left[\begin{array}{c} (Q_{ij}\cos\alpha_{ij} + F_{R\eta ij}\sin\alpha_{ij})\cos\varphi_j \\ +(T_{\xi ij} - F_{R\xi ij})\sin\varphi_j \end{array} \right] = m_i\ddot{y}_i, \tag{13}$$

$$F_z + \sum_{j=1}^{z} \left[\begin{array}{c} (Q_{ij}\cos\alpha_{ij} + F_{R\eta ij}\sin\alpha_{ij})\sin\varphi_j \\ +(T_{\xi ij} - F_{R\xi ij})\cos\varphi_j \end{array} \right] = m_i\ddot{z}_i,$$

$$M + \sum_{j=1}^{z} \left[\begin{array}{c} r_{ij}(Q_{ij}\sin\alpha_{ij} + F_{R\eta ij}\cos\alpha_{ij})\sin\varphi_j \\ +\frac{D_w}{2}r_{ij}T_{\xi ij}\sin\alpha_{ij}\cos\varphi_j \end{array} \right] = I_i\dot{w}_i. \tag{14}$$

where m_i is the mass of the bearing inner ring (kg); $\ddot{x}_i$, $\ddot{y}_i$, $\ddot{z}_i$ is the acceleration of the inner ring in the inertial coordinate system (m/s²); I_i is the inner ring moment of inertia; r_{ij} is the radial distance between the center of inner ring mass and the contact point of the raceway, T is the dragged force of bearing (N), F_R is the friction of bearing (N), Q is the contact force of the bearing (N).

(a) The relationship between inner ring and ball

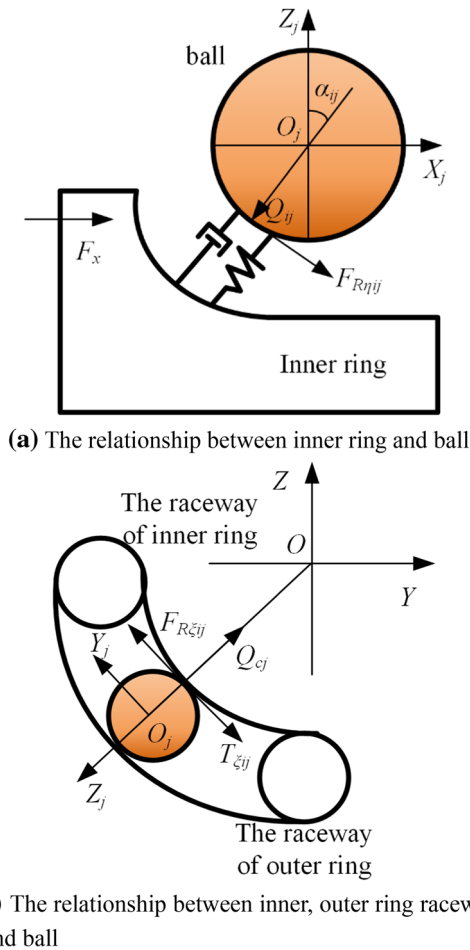**(b)** The relationship between inner, outer ring raceway and ball

Fig. 4 The forces between the inner, outer rings and the ball

According to the centrifugal displacement, dynamic displacement and thermal radial displacement of the bearing, the total displacement of the bearing is shown in Eq. (15).

$$
\begin{aligned}
\Delta f &= \Delta f_T + \Delta f_c + \Delta f_d \\
&= \Delta f_T + \Delta f_c + \sqrt{\Delta x^2 + \Delta y^2}.
\end{aligned}
\tag{15}
$$

where Δf_d is the dynamic displacement of bearing (μm), Δf is the total displacement of bearing (μm).

3 Interference fit discussion on spindle rotor system dynamic characteristics

The calculation of heat transfer coefficient are the important components in the spindle thermal boundary conditions [22]. The spindle is mainly divided into five parts to carry out the heat transfer coefficient. They are the end of the shaft convective heat transfer with surrounding air, heat transfer between the bearing and air, rotor convective heat transfer with compressed air, shell free convective heat transfer with

air and heat transfer of the cooling water and stator, respectively. Combined with the thermal boundary conditions of temperature field, considering the internal heat generating mechanism of spindle, the differential equation of energy conservation of motorized spindle is established by using finite element method, as is shown in Eq. (16) [23, 24].

$$
\rho_1 C_{p1} \frac{\partial T}{\partial t} + \rho_2 C_{p2} v \nabla T = \nabla(k \nabla T) + \frac{Q}{V},
$$
$$
\sum_{i=1}^{n=5} q_i = \sum_{i=1}^{n=5} h_i(T_f - T).
\tag{16}
$$

where ρ_1 and ρ_2 are the density of solid and fluid (kg/m³), C_{p1} and C_{p2} are the heat capacity of solids and fluid (J/kg °C), T is the temperature of spindle (°C), T_f is the temperature of the medium (°C), Q is the heat source (W), V is the volume of heat source (m³), v is the fluid velocity (m³/s), ∇ is the Laplace operator, k is the heat conductivity (W/m °C), h_i is the heat transfer coefficient (W/m² °C), q_i is the heat flux (J/m² s).

According to boundary conditions of temperature field, the 3D model of the spindle is imported into Comsol finite element software. And the stator, rotor, rotating shaft, cooling water channel and other core components are retained. In order to improve the accuracy and efficiency of temperature field calculation, some small grooves, threads and other complex parts are simplified. Meanwhile, the spindle model was divided into meshes, and the shape of meshes are mainly regular tetrahedral elements and triangular elements. The total number of spindle model elements is 206584, the number of the triangle elements is 37144, that of tetrahedral elements, edge elements and vertex elements are 165,062, 4064 and 314, respectively. In the meantime, the mass of the average and the minimum elements are 0.6537 g and 0.006606 g, and that the volume ratio of element is 3.594×10^{-11}.

4 Thermal displacement influence on spindle rotor system interference

The temperature field cloud diagram of the spindle rotor system is obtained by Comsol software, as shown in Fig. 5. It can be obtained that the temperature of the front bearing of the spindle rotor system is higher than that of the rear bearing. The rolling friction and sliding friction are relatively large due to the size of the bearing.

According to the temperature field model of the spindle rotor system, the relationship between the bearing temperature and speed is observed from Fig. 6.

The temperature of bearing has a non-linear relationship with the increasing speed. Meanwhile, the rate is continuously growing. The temperature of bearing rise gently under the speed of 3000–9000 rpm. And at the condition of the
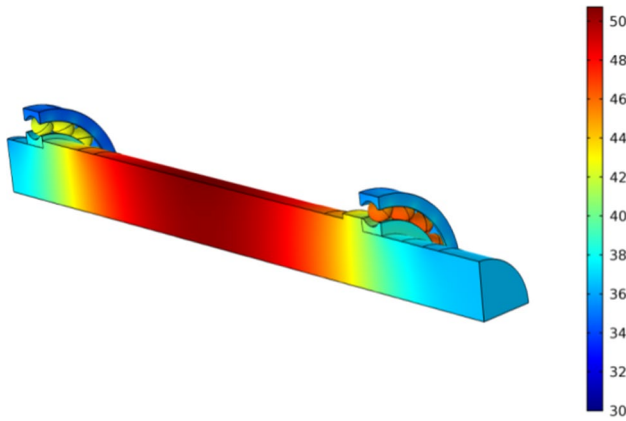
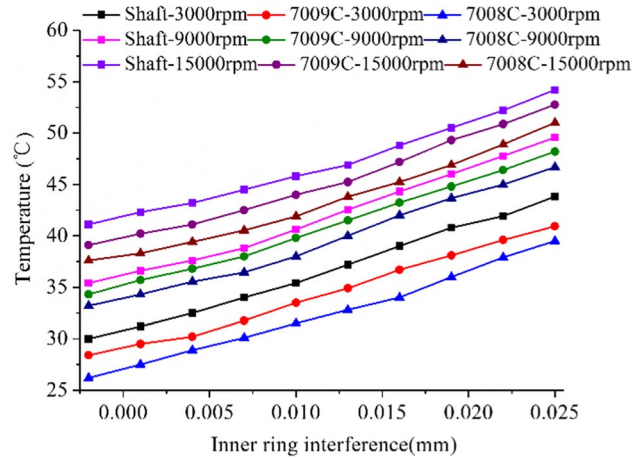**Fig. 5** The temperature field cloud diagram of the spindle rotor system

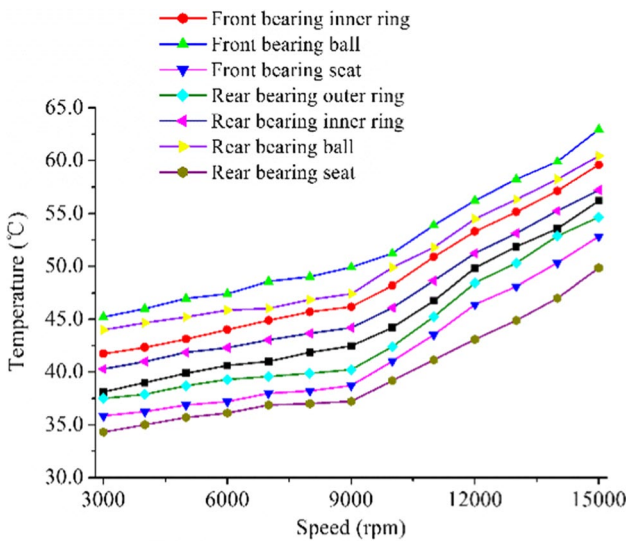**Fig. 7** The relationship between temperature and interference under different speed

Fig. 6 The relationship between temperature and rotational speed of front and rear bearings
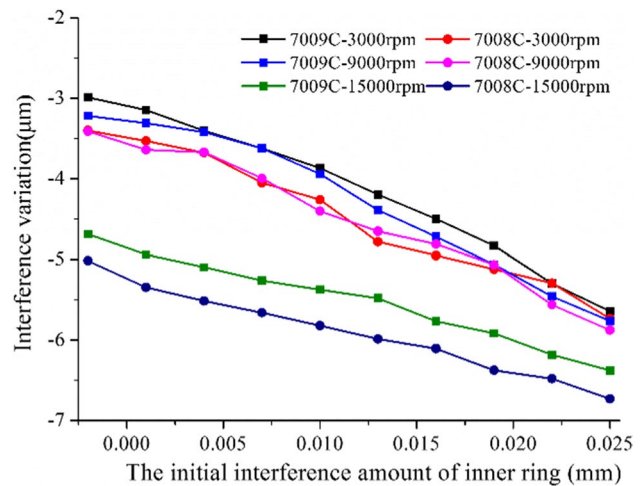

Fig. 8 Interference variation with the inner ring interference initial amount

speed is from 9000 rpm to 15,000 rpm, the slope of temperature rise greatly increases. Due to the size of the front bearing is larger, which lead to the friction and contact force becoming greater. It is obvious that the ball temperature is the highest part in the bearing. The inner ring, outer ring and the bearing seat are followed. The shaft transfers some heat to the inner ring through heat conduction, which eventually causes the temperature to be higher than that of the outer ring.

Figure 7 shows the relationship between temperature and interference under different speed. The matching pressure occurs a decreasing phenomenon that is derived from the interference increasing. The steady-state temperature of bearing becomes larger with the increasing of the inner ring initial interference. When the interference amount is

0.025 mm, the temperature of rotating shaft are 43.8, 40.9, 39.5 °C, the front bearing temperature are 49.8, 48.2, 46.7 °C, and the rear bearing temperature are 54.2, 52.8, 54 °C corresponding with the speed 3000, 9000 and 15,000 rpm respectively.

According to bearing interference model, the results in Fig. 8 show the interference variation with inner ring interference initial amount. It can be exhibited that the interference variation shows a nonlinear increasing trend with the initial interference amount becoming greater. Due to the thermal displacement of the shaft is always greater than bearing inner ring. The interference will become tighter, then it can lead to interference amount increasing. The thermal displacement has little influence on the interference variation before 9000 rpm. The thermal displacement rises rapidly after 9000 rpm, resulting in becoming greater of

interference variation. When the initial interference of the inner ring is 0.01 mm, the change of the front bearing inner ring interference variation are −3.15, −3.31 and −4.94 μm under 3000, 9000 and 15,000 rpm, respectively.

5 Centrifugal displacement influence on spindle rotor system interference

The centrifugal force is directly related to interference amount. The influence of centrifugal force on interference under different speed are calculated, as shown in Fig. 9.

With the speed becoming greater, the centrifugal displacement of the bearing inner ring and the shaft will increase. The centrifugal displacement of the bearing inner ring is always greater than the shaft, and it results in the reduction of interference fit. The trend of interference reduction amount presents rising phenomenon with speed. At 15,000 rpm, the maximum value of the bearing and shaft interference by centrifugal force is 13.7 and 2.4 μm. The interference amount of the rotor system is 11.3 μm.

6 Initial interference influence on spindle rotor system radial displacement

The dynamic displacement of bearing is calculated by applying Newton Raphson algorithm. The relationship between initial interference and dynamic radial displacement is obtained as shown in Fig. 10. With the increase of the initial interference of the inner ring, the dynamic radial displacement of the bearing inner ring decreases with small nonlinear trend. The dynamic radial displacement of 7008C bearing is smaller than that of 7009C bearing. When the
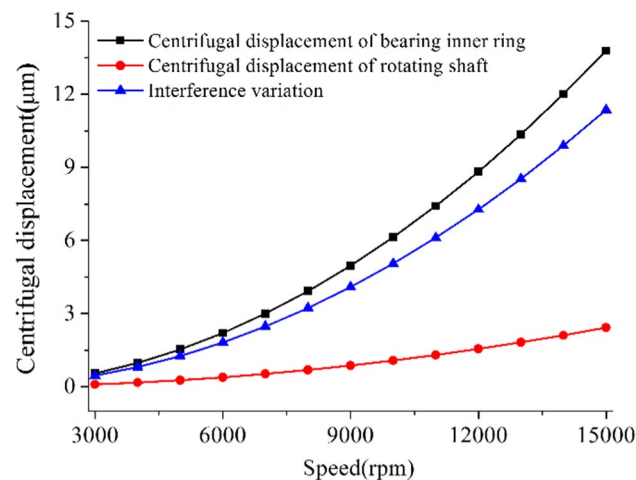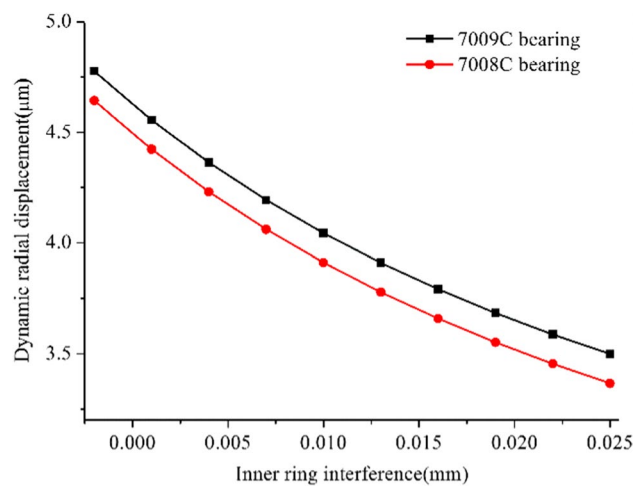

Fig. 10 The relationship between initial interference and dynamic radial displacement

interference is 0.025 mm, the radial displacement of the front and rear bearing inner rings are 3.51 and 3.38 μm, respectively.

Combined with the variation of the bearing displacement, the suitable interference amount is analyzed. Figure 11 shows the relationship between the bearing initial interference and dynamic radial displacement. There is an increasing nonlinear trend between radial displacement and speed. Before 9000 rpm, the bearings present a relatively stable state under the initial interference range of 0.004–0.007 mm. When the initial interference is greater than 0.007 mm, the radial displacement of the bearing presents an upward trend. With the inner ring initial interference increasing, there is an inflection phenomenon on the bearing radial displacement.
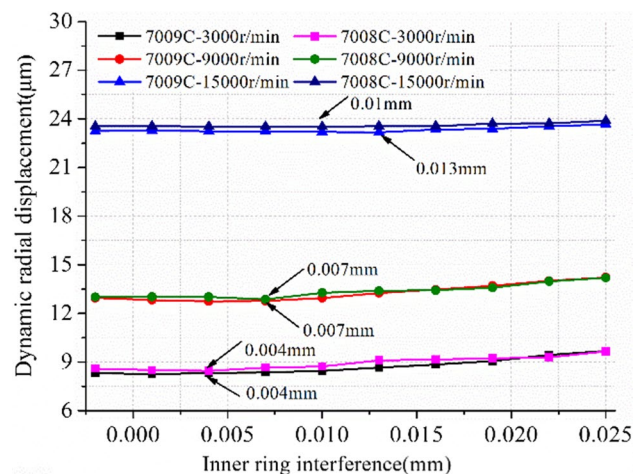

Fig. 9 The influence of centrifugal force on interference under different speed

Fig. 11 The relationship between the bearing initial interference and dynamic radial displacement

At the high speed condition, compared with the thermal displacement effect on the interference fit, the interference variation caused by centrifugal force is larger. The interference of front bearings are 0.004, 0.007, 0.013 mm that corresponds to the smaller bearing radial displacement 8.25, 12.74, 23.17 µm at 3000, 9000, 15,000 rpm, respectively. And the rear bearings are 0.004, 0.007, 0.01 mm corresponds to that of 8.45, 12.86 and 23.5 µm.

6.1 Interference amount influence on bearing vibration

Because the cage is not contact with bearing rings. Therefore, the influence of the force between ball and bearing inner, outer ring is much greater than that of the cage. In order to maintain the clarity of the bearing model, the influence of bearing cage is simplified [25]. A bearing dynamic model is established by the differential equation, for investigating the effect of the bearing interference amount on the bearing vibration, the equation of bearing is shown in Eq. (17).

$$m\ddot{x} + c\dot{x} + kx = me_0\omega^2 \cos \omega t - F_b\cos\theta,$$
$$m\ddot{y} + c\dot{y} + ky = me_0\omega^2 \sin \omega t + F_b\sin\theta - mg,$$
$$F_b = k \sum_{j=1}^{N} (\delta + \Delta f)_{ij}^{\frac{3}{2}}. \tag{17}$$

where m is bearing mass (kg), c is damping coefficient of bearing, k is the stiffness of bearing (Nm), δ_{ij} is contact deformation of ball and inner ring (µm), F_b is contact force of the bearing (N).
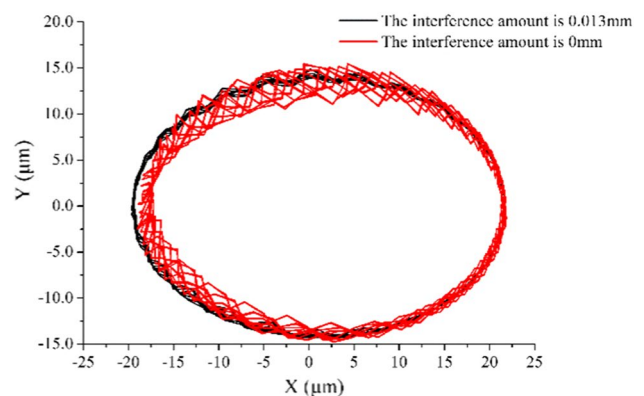
Newton iteration method is used directly to solve the differential equation in the paper. The vibration frequency domain diagram and vibration displacement diagram under different interference amount are shown in the Fig. 12.

The results exhibit when the bearing interference amount is variational, there is a significant effect on the bearing nonlinear dynamic behavior. It can be observed from Fig. 12a that the interference amount is 0.013 mm compared to that of 0 and 0.022 mm, the vibration velocity of one time frequency domain starts to emerge decreasing phenomenon at 15,000 rpm. The peak of the frequency domain amplitude are 3.76, 3.91 and 4.14 mm/s respectively. In addition to the basic frequency domain, the response of the bearing two times frequency domain is similar with that of one time frequency domain. Combined with the bearing interference fit model, the displacement variation caused by interference amount is the main factor of bearing vibration.

In order to analyze more about the dynamic characteristics of bearing, the vibration displacement of bearing is obtained in Fig. 12b. Due to the axial clearance of bearing, the displacement and fluctuation degree of X direction
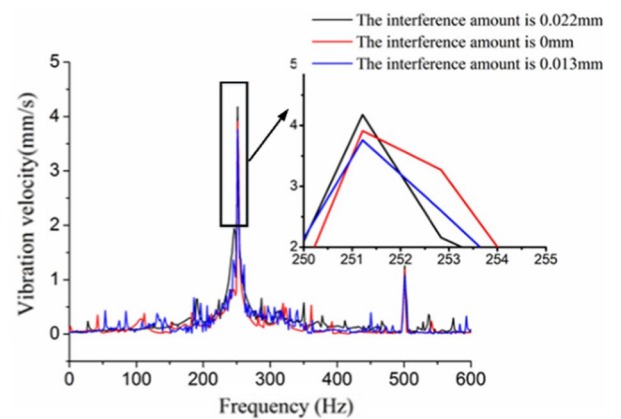
(a) The vibration frequency domain

(b) X,Y direction of vibration displacement

Fig. 12 The vibration frequency domain diagram and vibration displacement diagram under different interference amount

are greater than Y direction. From the results of vibration displacement distribution, the X, Y direction of Maximum displacement are 15.5 µm and 21.8 µm at the condition of the interference amount is 0 mm. which is greater than that of 0.013 mm. All of these exhibit that the dynamic behavior is mainly affected by bearing initial interference amount.

7 Experimental verification

The spindle is taken as an experimental object to verify the dynamic model in this paper. The spindle is installed on the experiment platform. The lubrication method of bearings is oil–gas lubrication. The temperature of the bearing outer ring is measured through Lion spindle error analyzer (SEA-5). In order to verify the accuracy of bearing dynamic model, the vibration experiment of spindle is designed. Due to the interference fit between the bearing inner ring and the rotating shaft, the dynamic characteristic of bearing inner ring is reflected by measuring the rotating shaft end. The shaft end vibration is tested by contactless laser vibration
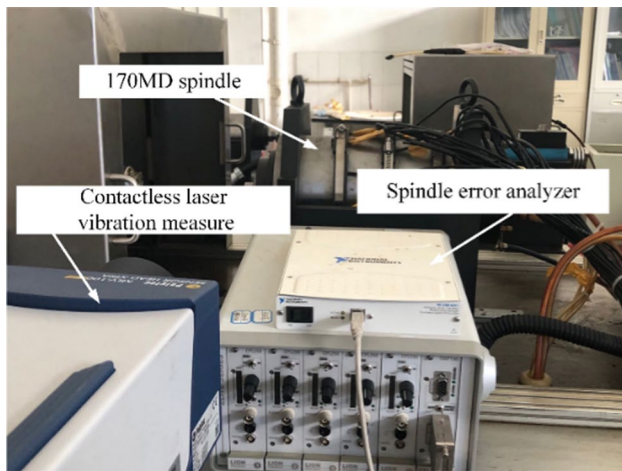
Fig. 13 The temperature and vibration experiment of spindle

Table 1 The specific parameters of the experiment

Parameter	Size
Front bearing	7009C
Rear bearing	7008C
Input oil	5 mL/h
Input air pressure	0.3Mpa
Bearing preload force	400 N
Cooling water temperature	16 °C
Cooling water flow rate	5 L/min
Environment temperature	20 °C
Logarithm of motor poles	2
Power	15KW

Fig. 14 The relationship of the bearing outer ring between the temperature and speed

(a) Vibration time domain

(b) Vibration frequency domain

Fig. 15 Comparison of vibration speed between bearing inner ring and spindle shaft

measure (Polytec5000-Xtra). The temperature and vibration experiment of spindle is shown in Fig. 13. The specific parameters of the spindle experiment is shown in Table 1 [26].

The spindle speed increases from 3000 to 15000 rpm. The relationship of the bearing outer ring between the temperature and speed is shown in Fig. 14. The outer ring temperature of the bearing shows an upward trend. The temperature of bearing increases slowly before 9000 rpm and rapidly after 9000 rpm. The maximum temperature difference between the simulation and the experiment of the front and rear bearing are 1.5 and 0.5 °C. This temperature model has good prediction accuracy for bearing temperature.

According to the bearing dynamic model, the vibration time–frequency domain simulation diagram of the front bearing is compared to the experiment, as shown in Fig. 15.

As shown in Fig. 15a, under the condition of 15,000 rpm, the experimental effective value of the rotating shaft vibration speed is basically the same as the simulated amplitude of the bearing inner ring, which is about 17.4 mm/s. There
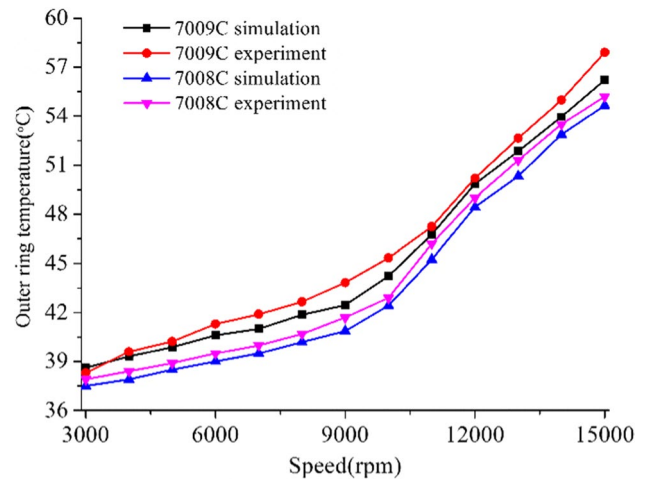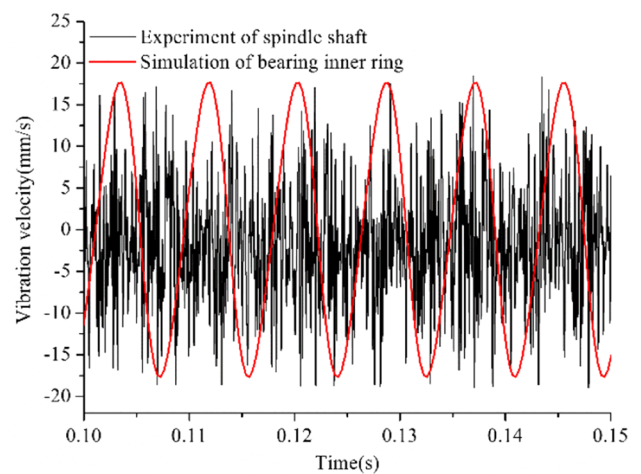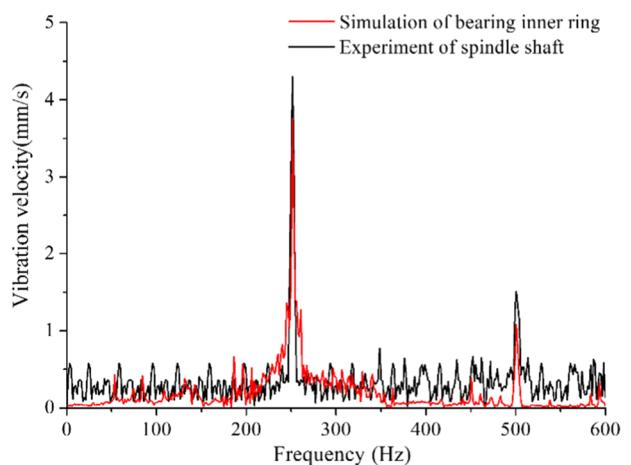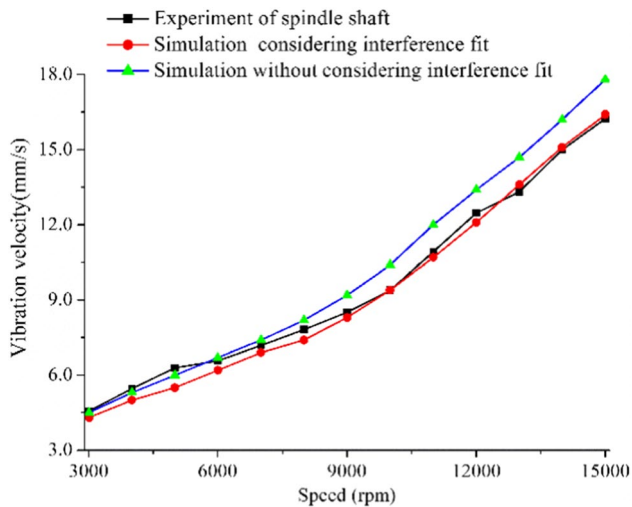
Fig. 16 The relationship between the experiment and simulation of bearing vibration velocity under different speed

is a certain error in the experimental value of the rotating shaft, which is mainly caused by the axial bearing preload and clearance. The frequency domain of vibration velocity comparison between the spindle shaft and the bearing is shown in Fig. 15b. Both the experimental and simulated frequency domain are about 250 Hz, and the amplitudes of one time frequency domain are 4.19 mm/s for the experiment and 3.87 mm/s for the simulation, respectively. The two times frequency is about 500 Hz, the error between the experimental amplitude and the simulated amplitude is 0.43 mm/s. The vibration amplitudes of the experiment and simulation are basically the same.

The relationship between the experiment and simulation of bearing vibration velocity under different speed is shown in Fig. 16. The vibration velocity shows an upward trend with increasing speed. The interference fit has obvious effect on the change of bearing dynamic displacement, resulting in the variation of bearing dynamic characteristics. Without considering interference fit, the maximum error between the simulation and the experiment is 1.55 mm/s at 15,000 rpm. Considering interference fit, the error is 0.15 mm/s, and the average error of theoretical values is 4.1%.

8 Conclusion

In this paper, a mathematical model of spindle rotor system is developed for spindle dynamic analysis in consideration of interference fit. The improved dynamic model for spindle rotor system is analyzed. The amounts of the interference fit are employed in the calculation. The validation experiments have also been carried out. The simulation

values of the model can match well with the experiment results. The conclusions of the paper are as follow:

(1) The presented dynamic model of the spindle rotor system is reliable to calculate the nonlinear dynamic behavior by considering the interference fit amount. The amount of interference fit is affected by temperature. Under different interference condition, the temperature distribution of bearing exhibits a nonlinear phenomenon through spindle thermal model. The average error of the model with temperature experiment is 2.6%.

(2) The dynamic and thermal influencing factors are involved in the bearing interference fit model, which the model reveals the dynamic radial displacement variation with interference amount. What is more, the centrifugal displacement and dynamic displacement influences on bearing interference amount are also significant.

(3) For a spindle operation, the relationship between the suitable interference fit and dynamic characteristics of rotor system is mainly determined. At low speed, the suitable interference of the front and rear bearings are 0.004 and 0.004 mm; at medium high speed, the suitable interference are 0.007 and 0.007 mm, respectively; and at high speed, the suitable interference are 0.013 and 0.01 mm, respectively. Under high speed, the interference of bearing and shaft should be appropriately increased, which is helpful to improve the dynamic characteristics of spindle.

The influence of interference fit on other complicated spindle rotor system will be focused in future studies. Its aim is to realize the applicable interference fit between shaft and bearings, thus to reduce the spindle deformation and improve the spindle dynamic characteristics during the spindle operation.

Availability of Data The data are available from the corresponding author on reasonable request.

Declarations

Conflict of interest The authors declared no potential conflicts of interest with respect to the research, authorship, and/or publication of this article.

References

1. Cao HR, Li BJ, Li YM, Kang T, Chen XF (2019) Model-based error motion prediction and fit clearance optimization for machine tool spindles. Mech Syst Signal Process 133:106252
2. Bhatti MM, Marin M, Zeeshan A, Abdelsalam SI (2020) Editorial: Recent trends in computational fluid dynamics. Front Phys 1:1–4
3. Tong VT, Hwang J, Shim JY et al (2020) Multi-objective optimization of machine tool spindle-bearing system. Int J Precis Eng Manuf 21:1885–1902
4. Raza R, Mabood F, Naz R, Abdelsalam SI (2021) Thermal transport of radiative Williamson fluid over stretchable curved surface. Thermal Sci Eng Progress 23:100887
5. Yan HP, Wu YH, li·SH et al (2020) Research on sound field characteristics of full-ceramic angular contact ball bearing. J Braz Soc Mech Sci Eng 42:311
6. Mao YZ, Wang LQ, Le GU (2016) Effect of negative clearance on dynamic characteristics of high-speed high-temperature thin-walled cylindrical roller bearings. J Aerospace Power 31:2795–2800
7. Liu GH, Hong J, Wu WW, Sun YH (2018) Investigation on the influence of interference fit on the static and dynamic characteristics of spindle system. Int J Adv Manufact Technol 99:1953–1966
8. Gruescu CM, Davidescu A, Carmen S, Lovasz E (2020) Interference fits. bearing capacity under complex loading—FEM analysis. New Adv Mech Mech Transmissions Robot, pp 403–414
9. Barmanov IS, Ortikov MN (2017) Ball bearing dynamics at the interference fit on balls. Proc Eng 176:19–24
10. Tsai JC, Chou TT, Chang CK (2020) Statistical analysis of contact stiffness for shaft-bearing assembly with tolerancing and fit. Procedia CIRP 92:45–50
11. Mao YZ, Wang LQ, Zhang C (2018) Influence of ring deformation on the dynamic characteristics of a roller bearing in clearance fit with housing. Int J Mech Sci 1:1–19
12. Chen SY, Kung CH, Liao TT, Chen YH (2010) Dynamic effects of the interference fit of motor rotor on the stiffness of a high speed rotating shaft. Trans Can Soc Mech Eng 34:243–261
13. Shi HT, Bai XT, Zhang K et al (2019) Effect of thermal-related fit clearance between outer ring and pedestal on the vibration of full ceramic ball bearing. Shock Vib 8357807:1–16
14. Bai XT, Zheng H, Wang ZN, Wang Z (2021) Raceway defect frequency deviation of full-ceramic ball bearing induced by fit clearance in wide temperature ranges. Shock Vib 6650798:1–13
15. Zuzana M, Petr B, Martin P (2018) Study of the press fit bearing-shaft joint dimensional parameters by analytical and numerical approach. Adv Mater Sci Eng 2916068:1–11
16. Guo TN, Ma XC, Gu YC, Chen JK (2016) Effect of the interference fit amount impact on the dynamic characteristics of spindle. J Beijing Univ Technol 42:51–59
17. Li G, Yuan H, Ma X (2014) Optimum design of the precise surface plate based on thermal deformation experiment and FEA. J Therm Stresses 37:1–13
18. Lee J, Kim DH, Lee CM (2015) A study on the thermal characteristics and experiments of high-speed spindle for machine tools. Int J Precis Eng Manuf 16:293–299
19. Wang YC, Kao MC, Chang CP (2011) Investigation on the spindle thermal displacement and its compensation of precision cutter grinders. Measurement 44:1183–1187
20. Wang ZN, Zhang K, Wang Z et al (2021) Research on vibration of ceramic motorized spindle influenced by interference and thermal displacement. J Mech Sci Technol 35:2325–2335
21. Xi ST, Cao HR, Chen XF (2019) Dynamic modeling of spindle rotor system and vibration response investigation. Mech Syst Signal Process 114:486–511
22. Bhatti MM, Alamri SZ, Ellahi R, Abdelsalam SI (2020) Intra-uterine particle–fuid motion through a compliant asymmetric tapered channel with heat transfer. J Therm Anal Calorim 144:2259–2267
23. Abdelsalam SI, Velasco-Hernández JX, Zaher ZA (2021) Electromagnetically modulated self-propulsion of swimming sperms via cervical canal. Biomech Model Mechanobiol 20:861–878
24. Zhang K, Wang ZN, Bai XT et al (2020) Effect of preload on the dynamic characteristics of ceramic bearings based on dynamic thermal coupling model. Adv Mech Eng 12(1):1–18
25. Cheng HC, Zhang YM, Lu WJ et al (2020) Research on the effect of structural and material parameters on vibrations based on quasi-static model of bearings. J Braz Soc Mech Sci Eng 42:578
26. Zhang LX, Li JP, Wu YH et al (2018) Prediction model and experimental validation for the thermal deformation of motorized spindle. Heat Mass Transfer, pp 1–14